

Journal Pre-proof

Mediterranean seascape suitability for *Lophelia pertusa*: Living on the edge

Fábio L. Matos, Joan B. Company, Marina R. Cunha



PII: S0967-0637(21)00035-2

DOI: <https://doi.org/10.1016/j.dsr.2021.103496>

Reference: DSRI 103496

To appear in: *Deep-Sea Research Part I*

Received Date: 1 June 2020

Revised Date: 28 January 2021

Accepted Date: 16 February 2021

Please cite this article as: Matos, F .L., Company, J.B., Cunha, M.R., Mediterranean seascape suitability for *Lophelia pertusa*: Living on the edge, *Deep-Sea Research Part I* (2021), doi: <https://doi.org/10.1016/j.dsr.2021.103496>.

This is a PDF file of an article that has undergone enhancements after acceptance, such as the addition of a cover page and metadata, and formatting for readability, but it is not yet the definitive version of record. This version will undergo additional copyediting, typesetting and review before it is published in its final form, but we are providing this version to give early visibility of the article. Please note that, during the production process, errors may be discovered which could affect the content, and all legal disclaimers that apply to the journal pertain.

  2021 Published by Elsevier Ltd.

1 Mediterranean seascape suitability for *Lophelia pertusa*: living on the edge

2 Fábio L. Matos^{1*}, Joan B. Company², Marina R. Cunha¹

3 ¹ CESAM - Centre for Environmental and Marine Studies, Department of Biology, University of
4 Aveiro, 3810-193 Aveiro, Portugal

5 ² Institut de Ciències del Mar (CSIC), Passeig Marítim de la Barceloneta, 37-49, 08003
6 Barcelona, Spain

7 * Correspondence:

8 Fábio L. Matos

9 fmatos@ua.pt

10 Abstract

11 Ecological niche modelling is used in deep-sea research to investigate the environmental
12 preferences and potential distribution of data-poor species. We present a mesoscale assessment
13 of Mediterranean seascape suitability for the cold-water coral *Lophelia pertusa* (= *Desmophyllum*
14 *pertusum*, Linnaeus, 1758). We estimated seascape suitability and uncertainty maps using an
15 ensemble approach of three machine-learning algorithms (Generalized Boosting Model, Random
16 Forest, Maximum Entropy) based on environmental predictors. Bathymetry, bathymetric slope
17 and pH were the most important predictors for the models. Overall the models reached good to
18 excellent performance, with a very reliable prediction of the most suitable areas. In the
19 Mediterranean Sea, *L. pertusa* encounters environmental settings close to its physiological limits
20 but, despite the highly variable quality of the Mediterranean seascape, we identified high
21 suitability areas mostly along the upper slope and at submarine canyons of the Western and
22 Central margins. The existing MPAs do not overlap with high suitability areas, and therefore *L.*
23 *pertusa* is only protected at the deepest fringe of its potential distribution by the implementation
24 of the bottom trawling exclusion beyond 1000 m depth. This seascape suitability assessment
25 may assist future research, including high-resolution modelling targeting high-suitability areas,
26 investigation on the resilience of *L. pertusa* populations and development of conservation
27 actions.

28 **Keywords:** Cold-water corals; potential distribution; climate change; conservation; ensemble model

29 1 Introduction

30 The geographical distributions of species in the deep sea remain largely unknown. This
31 knowledge deficit has hindered the development of effective management measures framed by
32 recent policy initiatives (e.g., European Habitats and Marine Strategy Framework Directives) that
33 aim to preserve the biodiversity and functioning of ecosystems. Conservation options heavily rely

34 on spatial explicit information (Reiss et al., 2015; Savini et al., 2014) and depend on modelling
35 approaches at broad spatial scales (Burgman et al., 2005). This methodology allows capturing
36 the multiple interactions between the organisms and their habitats and the spatio-temporal
37 dynamics of the landscape (Turner et al., 1995). The mapping of areas with suitable conditions
38 for the settlement of habitat forming species such as some cold-water corals (CWC) is an
39 important aspect of conservation and management of deep-sea biodiversity.

40 Cold-water corals are among the most emblematic deep-sea organisms and play an important
41 role in the structure and functioning of marine ecosystems. CWC increase the complexity of the
42 habitat, provide spawning, nursery and feeding areas and support attendant assemblages with
43 significantly enhanced biodiversity and biomass when compared to the surrounding environment
44 (Buhl-Mortensen et al., 2010; Capezzuto et al., 2018; Corbera et al., 2019; Linley et al., 2017).
45 CWC are also involved in the provision of other important ecosystem functions and services
46 (Giovanni Chimienti and D'Onghia, 2019) including nutrient cycling and carbon sequestration
47 (Soetaert et al., 2016). Due to their low tolerance to disturbance (low resistance), slow growth
48 rates (low recovery rates), and consequently poor resiliency, these organisms can be highly
49 impacted by anthropogenic activities (D'Onghia et al., 2017; Fabri et al., 2017; 2014; Giusti et al.,
50 2019; Taviani et al., 2019a) and climate change (Georgian et al., 2016; Movilla et al., 2014).

51 Among the reef-building CWC species, *Lophelia pertusa* is one of the most studied. Classified as
52 deep-sea cosmopolitan along the western and eastern margins of the North Atlantic Ocean
53 (Roberts et al., 2016), it is also widely reported from the Gulf of Mexico and the Caribbean Sea
54 and in many mid-ocean islands (Rogers, 1999). In the Mediterranean Sea, there are many
55 records of dead or subfossil remains, mostly dated from the late Pleistocene, 30000-15000 years
56 B.P. (Delibrias and Taviani, 1985). Climate change that marked the end of the last glacial period,
57 and its influence on patterns of productivity and deep-sea water circulation are hypothesized as
58 the causes for a major decline of the once thriving Mediterranean populations (Delibrias and
59 Taviani, 1985; Fink et al., 2015; Taviani et al., 2019b). Reports of presently living colonies in the
60 Mediterranean Sea are few and restricted to the western-central Mediterranean basin (Chimienti
61 et al., 2018; 2019). However, taking into account that few surveys targeting *L. pertusa* were
62 conducted in the Mediterranean Sea and, nonetheless, several recent studies reported new
63 occurrences of living colonies (e.g., Angeletti et al., 2014; Corbera et al., 2019; Taviani et al.,
64 2019a), the present Mediterranean distribution of *L. pertusa* is probably underestimated
65 (Zibrowius, 2003).

66 Recent studies have successfully used ecological niche models (ENMs) to estimate the potential
67 distribution and the environmental suitability of various deep-sea species (e.g., Basher et al.,
68 2014; Davies and Guinotte, 2011; González-Irusta et al., 2015; Lo-lacono et al., 2018). The
69 panoply of ENMs available encompasses different approaches, modelling techniques,
70 occurrence data inputs, and ecological concepts (Peterson et al., 2015; Valverde et al., 2008).

71 Correlative ENM forecasts based on presence-only data rely on a set of ecologically relevant
72 predictors and provide meaningful results even for poor-data species. The modelling process
73 consists in determining statistically the species environmental profile based on the values of
74 predictors for the known occurrence locations and then project this profile over the model's
75 geographical space (Guillera-Arroita et al., 2015; Miller, 2010). The output is a continuous
76 representation of the species potential distribution. Model predictions depend not only on the
77 adopted modelling technique and settings defined by practitioners but are also subject to
78 different types of uncertainties related to data quality and quantity (e.g., sample size, sampling
79 bias, spatial resolution issues (Burgman et al., 2005; Zhang et al., 2015)). These issues and their
80 implications on the model performance have prompted the use of ensemble forecasting
81 frameworks that combine the output of multiple models into a single estimation. This
82 methodology produces frequently more accurate predictions than single model methods (Turner
83 et al. 2018) and allows highlighting consensual forecasts by mapping model uncertainty based
84 on the agreement/disagreement of individual models (Araújo and New, 2007).

85 The main objective of this work is to predict and map the Mediterranean seascape environmental
86 suitability for *L. pertusa* using a multiple model ensemble forecasting approach that can provide
87 support for management decisions and conservation actions. We provide here a succinct and
88 easily readable potential distribution map, assess the performance of the model and derive the
89 prediction uncertainty maps for the modelled geographical area. We also hypothesize that *L.*
90 *pertusa* in the Mediterranean Sea is subjected to conditions near its physiological tolerance and
91 that its persistence in this region is being challenged by climate change. To our best knowledge,
92 this study is the first focusing on assessing the seascape suitability for *L. pertusa* in the
93 Mediterranean Sea, encompassing the whole basin and using a multi-algorithm approach that
94 provides both the prediction of seascape suitability and a measure of uncertainty of the forecast.

95 2 Material and methods

96 2.1 Modelling area and occurrence data

97 We modelled the seascape suitability of the Mediterranean Sea for *L. pertusa* using present-day
98 living occurrences reported for the study area. We extracted the occurrence records in the
99 Mediterranean Sea from the Global Distribution of Cold-water Corals Database (version 3.0,
100 Freiwald et al., 2017), further updated with records for the Mediterranean Sea obtained from the
101 literature (Supplementary Table S1). We excluded colony records referring to transects covering
102 a distance greater than 230 m to reduce the geographic uncertainty of the occurrence data. For
103 shorter transects (8 out of 48), we considered the centroid of the transect as the location of the
104 colony. Considering the modelling resolution (1/8 arc minute, ca. 230 × 230 m), this lack of
105 accuracy was assumed as negligible. To remove duplicates and spatially auto-correlated
106 occurrences, we proceeded with the spatial thinning of species occurrences (Aiello-Lammens et
107 al., 2015), that reduced multiple occurrences within 230 m radius to a single record. This
108 procedure minimizes the sampling bias and prevents the over-fitting of predictions without losing
109 an excessive amount of information.

110 2.2 Environmental predictors

111 We based the selection of environmental predictors (Table 1) on the species ecology and
112 previous modelling studies for *L. pertusa*. The bathymetry (meters) was extracted from the
113 EMODnet Digital Bathymetry dataset and used to derive the bathymetric slope (degrees). Seven
114 predictors related to ocean conditions were extracted from data assimilative ocean models
115 available through the Copernicus Marine Environment Monitoring Service (CMEMS): salinity
116 (psu), temperature (°C), dissolved oxygen (mmol m^{-3}), phosphate concentration (mmol m^{-3}),
117 phytoplankton carbon biomass (mmol m^{-3}), pH and current velocity (m s^{-1}). We used a
118 continuous representation of near seafloor conditions for these variables following the
119 methodology described by Davies and Guinotte (2011) but using kriging instead of inverse
120 distance weighting as the interpolation method. This option was based on studies showing higher
121 performance for the first method (Assis et al., 2018; Hofstra et al., 2008). The fitting of the
122 universal kriging model was based on the 12 nearest values of each focal cell. The assessment
123 of the up-scaling process of the environmental data was conducted using the data provided by
124 the World Ocean Atlas 2013 (WOA 2013, version 2, E. H. Garcia et al., 2013; H. E. Garcia et al.,
125 2013; Locarnini et al., 2013; Zweng et al., 2013). Only the values of the WOA 2013 deeper than
126 50 m were retained for the assessment of the quality of the interpolation process and compared
127 with the interpolated data layers with the closest depth. Relationships were statistically analyzed
128 using the Pearson's correlation coefficient. The predictors' covariance was also assessed; the
129 bathymetry and pH were highly correlated ($r = 0.86$, Supplementary Fig. S1) however, we opted
130 to retain both predictors since: 1) the bathymetry is frequently identified as one of the most

131 relevant predictors to estimate the environmental suitability for CWC in regional studies (e.g.,
 132 Barbosa et al., 2019; Georgian et al., 2014); 2) the pH level is particularly relevant under the
 133 current state of ocean acidification (Hennige et al., 2014).

134 Table 1 – Details of the environmental predictors used in the model fitting and respective sources.

Variable (units)	Native Resolution	Derived from	Source	Reference
Bathymetry (m)	0.002°		EMODnet Digital Bathymetry (DTM 2016)	EMODnet Bathymetry Consortium, 2016
Bathymetric slope (°)		Bathymetry		
Phytoplankton carbon biomass - PCB (mmol m ⁻³)				
Phosphate (mmol m ⁻³)	0.063°		Mediterranean Sea Biogeochemistry Reanalysis - CMEMS	Teruzzi et al., 2019
pH				
Dissolved O ₂ (mmol m ⁻³)				
Salinity (psu)				
Temperature (°C)	0.063°		Mediterranean Sea Physics Reanalysis - CMEMS	Simoncelli et al., 2019
Current velocity (m s ⁻¹)				

135

136 The modelling process was conducted using R (R Core Team, 2016) and the “Biomod2”
 137 package (Thuiller et al., 2009) – version 3.3-15) which supports different modelling techniques.
 138 The ensemble model output resulted from the consensus of three machine-learning algorithms:
 139 Generalized Boosting Model (GBM, also known as Boosted Regression Trees), Random Forest
 140 (RF), and Maximum Entropy (MaxEnt). The machine-learning class algorithms are among the
 141 most appropriate for mapping and discriminating areas with different suitability degrees while
 142 keeping a high predictive performance (Carvalho et al., 2017; Mi et al., 2017; Reiss et al., 2015;
 143 Scales et al., 2016). Moreover, the predictions of these algorithms are considered more robust to
 144 predictors’ correlations (Anderson et al., 2016) and to issues related to sample size (Hernandez
 145 et al., 2006; Mi et al., 2017; Wisz et al., 2008). They are also adequate for handling complex
 146 interactions between species response and predictor variables (Wisz et al., 2008).

147 The selected algorithms require pseudo-absence or background information for building the
 148 models. We generated ten datasets with 100 randomly sampled pseudo-absences each for GBM
 149 and RF algorithms, following the recommendations by Barbet-Massin *et al.* (2012). A minimum
 150 distance of 10 km from any presence point was imposed using the geographical constraint
 151 strategy offered in “Biomod2” to avoid pseudo-replicates. Considering the nature of MaxEnt
 152 (Philips and Miroslav, 2008), the procedure applied to the models using this algorithm differed
 153 slightly from the previous – 10000 random background points were selected to reach the optimal
 154 performance of the algorithm, and no geographic constraints were applied. Although a sampling

155 bias correction in the selection of the background data for MaxEnt models is recommended
156 (Philips and Miroslav, 2008), this procedure was hindered by the paucity of publicly available
157 data for the Mediterranean Sea that affects the current knowledge regarding *L. pertusa*
158 distribution. The adjustment of the model complexity is also recommended by Merow (2013) but
159 we maintained the default settings supplied by “Biomod2” because of the lack of truly
160 independent evaluation data for model tuning. The tuning process is fundamental for models
161 aiming high transferability (i.e., to be projected to other areas or periods) but it is less important
162 in studies aiming to project the prediction of the model to the same area used for its calibration
163 (Anderson and Gonzalez, 2011). We weighted equally each observation (either presence or
164 pseudo-absence/background point) during the calibration process.

165 2.2.1 Evaluation of models' performances

166 A total of 300 single models were generated resulting from ten runs of the three algorithms for
167 the ten datasets using either pseudo-absences (GBM and RF) or background points (MaxEnt).
168 The evaluation of the models was performed by splitting the original datasets randomly into two
169 subsamples: 75% of the data were selected for the calibration of the models, and the remaining
170 25% were used to test their predictions. This procedure was repeated 10 times using the method
171 implemented in “Biomod2”, similar to a cross-validation procedure. This method results in a quite
172 robust test of the model performance in the absence of independent data (Thuiller et al., 2009).

173 There is no consensus on the most appropriate metrics to assess the accuracy of a model and,
174 instead, a multi-metric approach is encouraged. We chose three of the most commonly used
175 metrics: the area under the curve of the Receiver Operator Characteristic (ROC), the True Skill
176 Statistic (TSS), and the Boyce Index. The ROC is a threshold independent metric, neutral to
177 species prevalence, which measures the discrimination capacity regarding relative proportions of
178 correctly and incorrectly classified predictions (Pearce and Ferrier, 2000). The ROC values range
179 from 0 to 1, with 1 corresponding to a perfect classification. The TSS is also independent of the
180 species prevalence and compares the number of correct predictions subtracted by those
181 assigned by chance in a perfect theoretical forecast (Omri et al., 2006); this statistic ranges from
182 -1 to 1, with values near 1 indicating a good agreement between predictions and observations.
183 The Boyce Index (Boyce et al., 2002; Hirzel et al., 2006), calculated separately using the
184 “ecospat” package (Di Cola et al., 2017) for R, is a threshold independent evaluator ranging also
185 from -1 to 1. Values close to 1 indicate a good agreement between the model predictions and the
186 presences distribution in the evaluation dataset, i.e., areas with a high number of occurrences
187 are scored with high suitability values (Hirzel et al., 2006). Conversely, values close to -1 indicate
188 that areas with a high number of occurrences are scored with low suitability values, and thus the
189 model performed poorly. Values close to zero indicate that the model is not different from a
190 random forecast. For each algorithm, we calculated the mean of each metrics.

191 The contributions of the variables to the models can differ between algorithms and between runs.
192 We estimated the importance of each predictor using a randomization procedure. We used the
193 built-in method in “Biomod2” that uses Pearson correlation between the standard predictions and
194 the predictions where the variable of interest has been randomly permuted. If the correlation
195 value between the two predictions is high, the variable permuted is considered not important
196 for the model prediction. This method is independent of the modelling techniques and thus allows
197 direct comparisons between models (Thuiller et al., 2009). This procedure was repeated ten
198 times for each predictor during the modelling process.

199 2.2.2 Ensemble modelling

200 Ensemble forecasting was performed by combining a subset of the single models. Only models
201 with a TSS equal or greater than 0.8 were retained to build the consensus maps. As for the
202 evaluation of models, there is no consensus on the most appropriate metric to select the single
203 models used to build the ensemble model (Scales et al., 2016). However, the TSS and the ROC
204 are among the metrics most frequently used. We opted to use the TSS over the ROC because
205 the reliability of the latter has been heavily criticized (Lobo et al., 2008).

206 We combined the habitat suitability values of each grid cell using three consensus algorithms
207 (Thuiller et al., 2009): 1) the mean of the probabilities over the selected models; 2) the binary
208 models' committee averaging; and 3) the coefficient of variation of probabilities. The first
209 algorithm provides the prediction of seascape suitability while the other two provide a measure of
210 uncertainty of the predictions.

211 The ensemble model based on the mean of probabilities of the selected models ($TSS \geq 0.8$) is a
212 continuous representation of the habitat suitability index (HSI) ranging from 0 to 1000, with
213 values close to 1000 representing the most suitable areas. The committee averaging returns the
214 average of binary prediction (transformation of the models' output to presence/absence
215 estimations) based on a threshold that maximises the values of TSS; it gives both a prediction
216 and a measure of uncertainty. Values close to 1 or 0, mean that all models agree to predict
217 presence and absence, respectively, while values around 0.5 correspond to the highest
218 uncertainty in the predictions. The coefficient of variance (i.e., standard deviation/mean of
219 probabilities) can also be used as a measure of the model uncertainty: lower scores correspond
220 to better predictions and higher scores to higher levels of uncertainty.

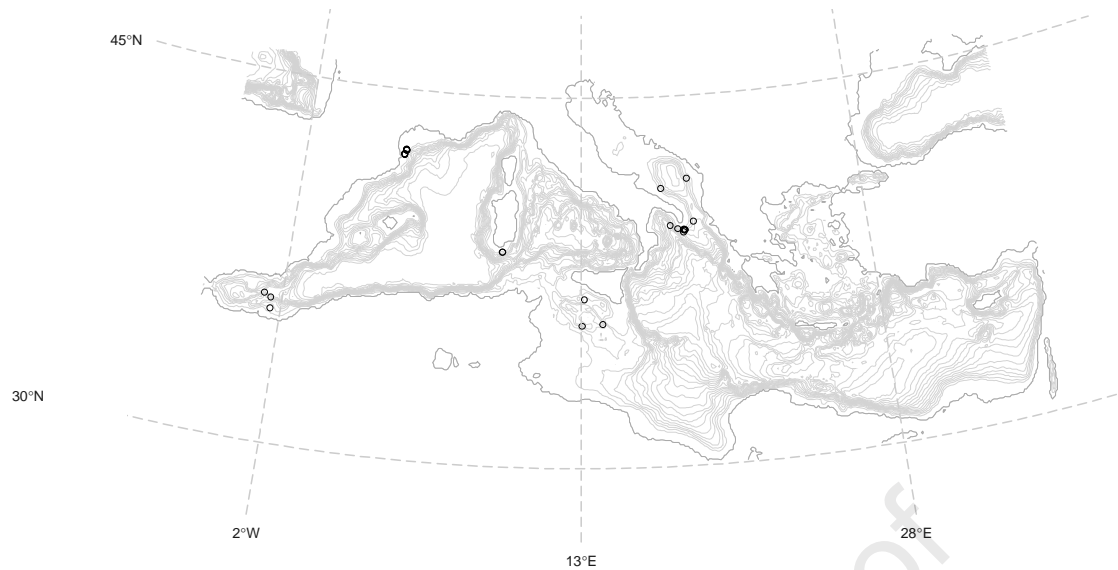
221 To rank the seascape features in the Mediterranean Sea by suitability, we intersected the output
222 of the mean ensemble model with the seafloor geomorphological classification produced by
223 Harris *et al.* (2014), the authors used the nomenclature defined, primarily, by the International
224 Hydrographic Organization for the seafloor feature types. According to the terminology used by
225 Harris *et al.* (2014), and references therein) we identified the following features in the
226 Mediterranean Sea:

- 227 • Shelf valleys - features incising the continental shelves or intersecting the shelf breaks no
228 longer than 10 km in length.
- 229 • Terraces on the continental slope - “isolated or group of relatively flat horizontal or gently
230 inclined surfaces, sometimes long and narrow, which are bounded by a steeper ascending
231 slope on one side and by a steeper descending slope on the opposite side”.
- 232 • Continental rise - identifiable by the occurrence of a smooth sloping seabed adjacent to the
233 base of the continental slope, in general, with a sediment layer > 300 m thick.
- 234 • Sills - “seafloor barriers of relatively shallow depth restricting water movement between
235 basins”.
- 236 • Seamounts - “discrete or group of large isolated elevations, greater than 1000 m in relief
237 above the sea floor, characteristically of conical form”.
- 238 • Guyots or tablemounts - “isolated or group of seamounts having a comparatively smooth flat
239 top”.
- 240 • Submarine canyons - “steep-walled, sinuous valleys with V-shaped cross sections, axes
241 sloping outwards as continuously as river-cut land canyons and relief comparable to even the
242 largest of land canyons”.
- 243 • Ridges - “isolated or group of elongated narrow elevations of varying complexity having steep
244 sides, often separating basin features”.
- 245 • Troughs: “long depressions of the sea floor characteristically flat-bottomed and steep sided
246 and normally shallower than a trench”.
- 247 • Trenches: “long narrow, characteristically very deep and asymmetrical depressions of the sea
248 floor, with relatively steep sides”.
- 249 • Bridges - blocks of material that partially infill trenches and troughs.
- 250 • Fans - “relatively smooth, fan-like, depositional features normally sloping away from the outer
251 termination of a canyon or canyon system”.

252 Additionally, we used the MPAtlas database of the Marine Conservation Institute
253 (www.mpatlas.org) to analyze the overlap between areas of suitability and the existing marine
254 protected areas (MPAs) in the Mediterranean Sea.

255 **3 Results**

256 We estimated the environmental suitability of the seascapes for *L. pertusa* in the Mediterranean
257 Sea. A total of 30 occurrences of living colonies sparsely distributed across the western and
258 central Mediterranean basins were used in our model (Fig. 1). No records of living colonies of *L.*
259 *pertusa* were reported in the literature for the eastern Mediterranean Sea.



260

261
262

Fig. 1 - The distribution of the living colonies of *L. pertusa* in the Mediterranean Sea used in the ecological niche model.

263

3.1 Environmental profiling

264

265

266

267

268

269

270

271

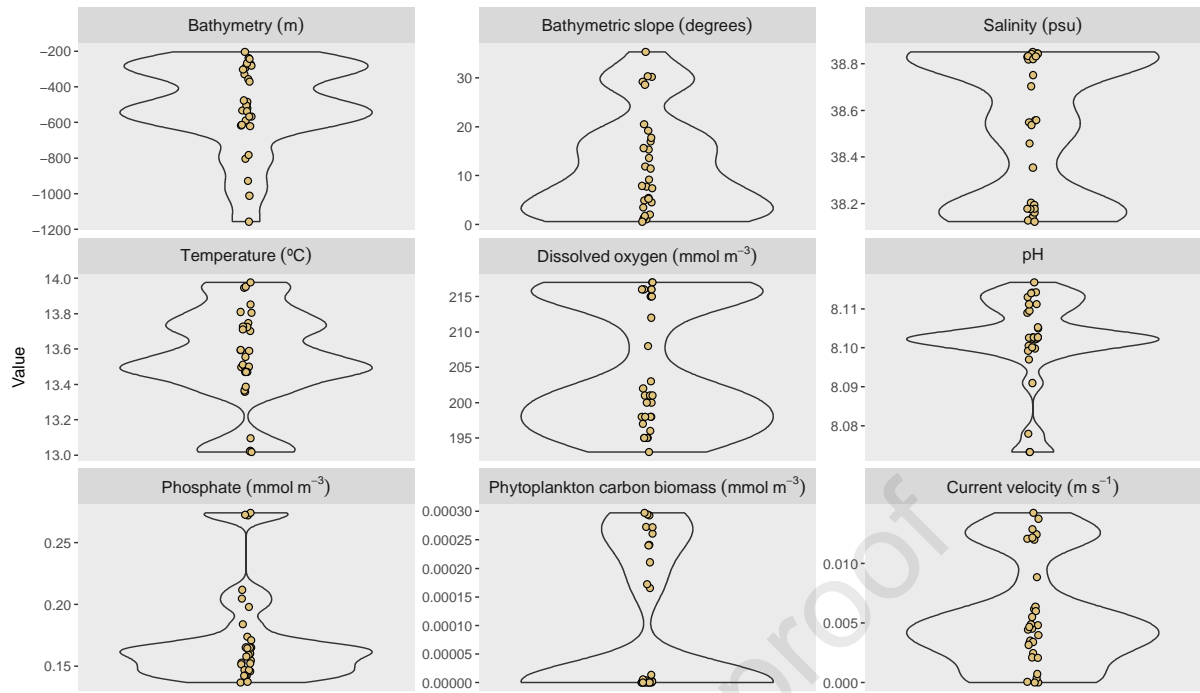
272

273

274

275

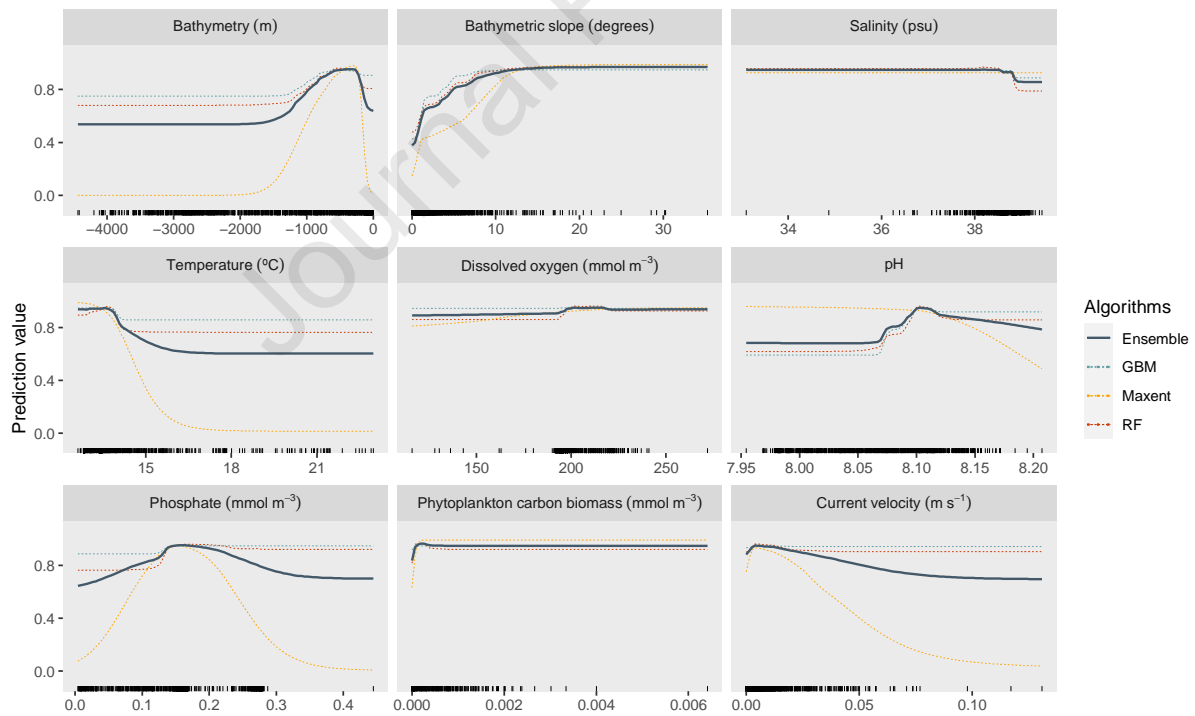
The intersection of the record of presences with the values of the environmental predictors (Fig. 2) illustrates how the species distribution is related to these variables. On the other hand, the response curves (Fig. 3) describe the suitability variation along the observed range of values for the different predictors. The MaxEnt models returned the most complex behavior but possibly the best representation of the species response to the extremes of environmental gradients (with predicted responses close to zero, Fig. 3). The GBM and RF models showed smoother response curves and similar trends, but lower sensitivity to the environmental gradient variation. The response curves of the ensemble model combine the responses of the selected single models. The colonies of *L. pertusa* were mainly concentrated at depths between 200 and 620 m and in gentle slope areas. According to our model (Fig. 3), suitability is high between 180 and 950 m and peaks at depths close to 300 m; it also rises progressively with increasing slope and maintains high values at slopes $>8^\circ$.



276

277
278

Fig. 2 - Violin plots showing the distribution of the species occurrences (white area illustrates the relative frequency of occurrence) intersected with the environmental predictors.



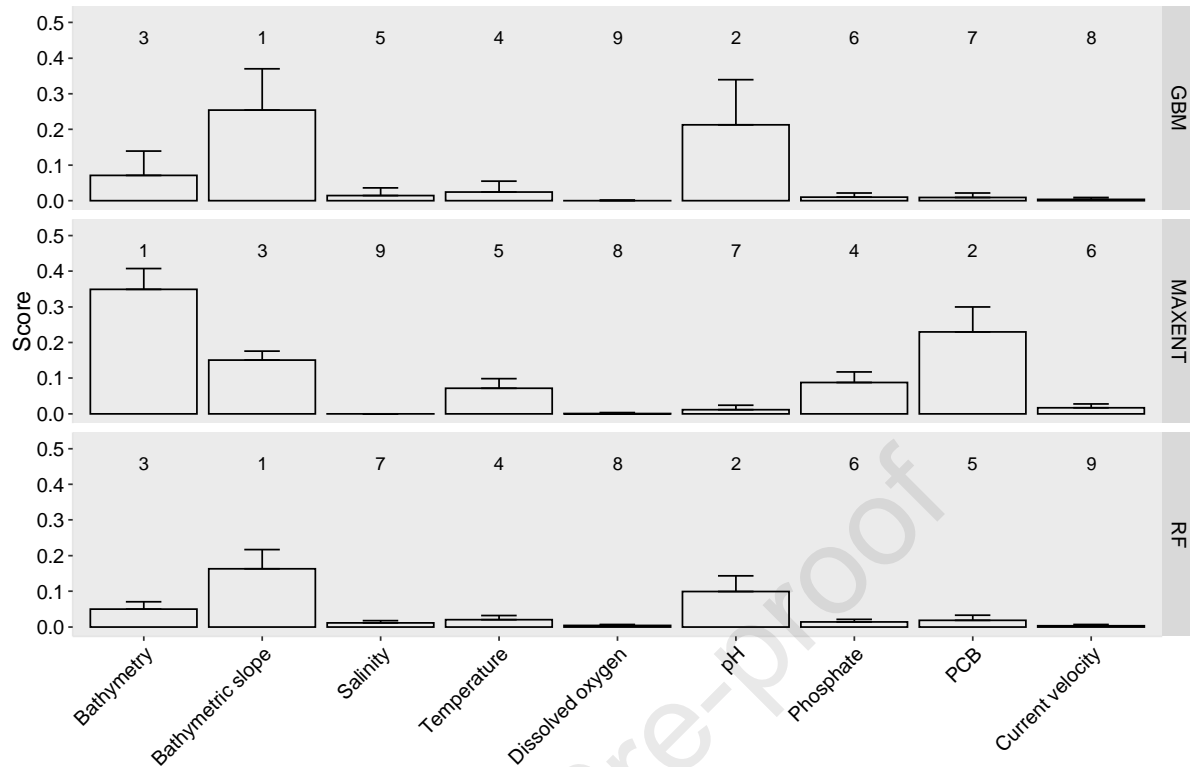
279

280
281
282
283
284
285

Fig. 3 - Univariate response curves for each environmental predictor according to the mean ensemble model (solid line) and the average response of single models (dashed lines) according each algorithm. The variables environmental gradients are represented in the x-axis and the suitability prediction values in the y-axis. The shaded areas correspond to the range of values observed for the single models according to each algorithm. The rug lines (x-axis) correspond to the data points of the *L. pertusa* occurrences and pseudoabsences used in the models' fitting.

286 The occurrences of *L. pertusa* in the Mediterranean Sea were concentrated at temperatures
287 between 13-14 °C and salinity values ranging from 38.1 to 38.8 (Fig. 2). Values beyond these
288 intervals result, according to the ensemble model, in a decrease in the environmental suitability
289 for the occurrence of *L. pertusa* colonies in the modelling area (Fig. 3). The colonies were
290 detected at concentrations between 193-217 mmol m⁻³ of dissolved oxygen (DO), with values
291 greater than 197 mmol m⁻³ offering more suitable conditions for the species occurrence (Fig. 3).
292 All colonies were subject to pH levels ranging from 8.07 to 8.12 and phosphate concentrations of
293 0.14-0.27 mmol m⁻³ (Fig. 2). Values out of these ranges result in the decrease of the
294 environmental suitability for the species occurrence in the Mediterranean Sea (Fig. 3). The live
295 colonies of *L. pertusa* were subjected to very low concentration of the phytoplankton carbon
296 biomass and to current velocities lower than 0.014 m s⁻¹ (Fig. 2). The increase of the current
297 velocity results in a progressive reduction in the environmental suitability of the species
298 occurrence (Fig. 3).

299 The contributions of the variables to the predictions differ between algorithms (Fig. 4). The
300 bathymetric slope, pH and bathymetry showed, in this order, the highest contributions in GBM
301 and RF estimates, while bathymetry, phytoplankton carbon biomass and bathymetric slope were
302 the most relevant contributors for MaxEnt estimates. On the other hand, DO, current velocity,
303 and salinity were amongst the least important contributors to models' estimates. The variables'
304 contributions to the ensemble model are not presented because this model is composed of a
305 combination of the results from different algorithms and therefore such contributions cannot be
306 interpreted in a meaningful way (Aguirre-Gutiérrez et al., 2013).

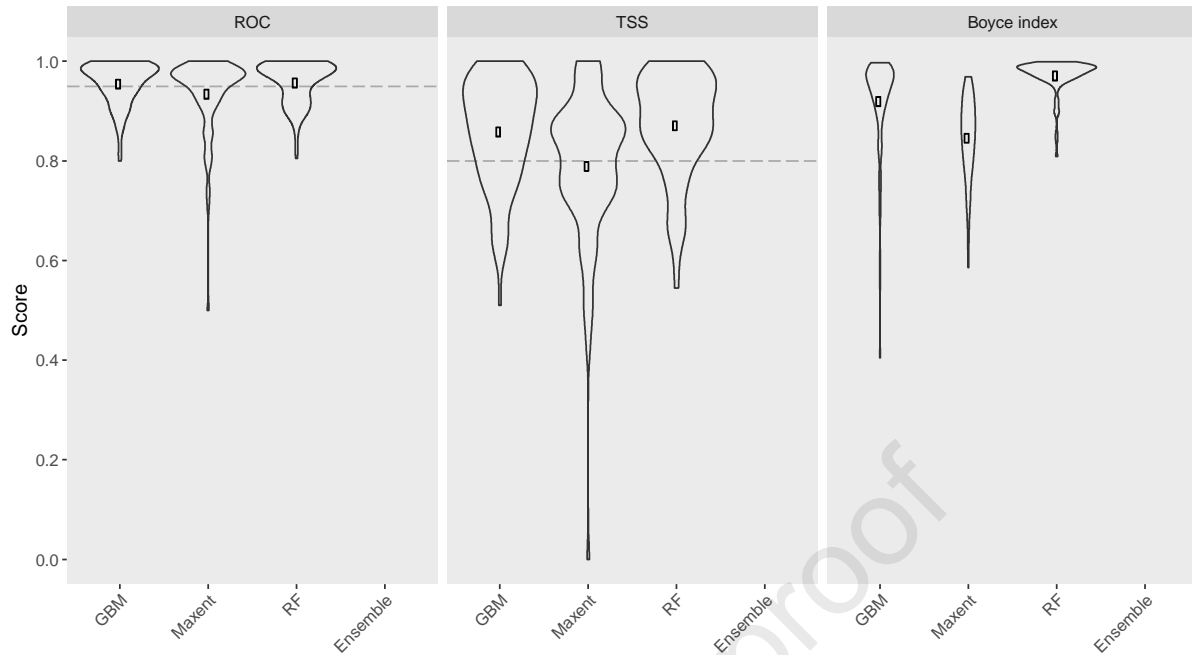


307

308 Fig. 4 - Predictors contributions scored as the relative importance to models considering all pseudo-absence
 309 datasets and evaluation runs by algorithm (ranging between 0 and 1). The higher the value, the more important
 310 the variable is to the model, while the value zero means no influence at all. The interaction between predictors
 311 was not considered.

312 3.2 Performance of the models

313 The performance of the models was assessed using ROC, TSS and Boyce index (Fig. 5). ROC
 314 values greater than 0.95 and TSS scores equal or greater than 0.8, were considered highly
 315 accurate. According to the different metrics, the GBM and RF models reached good to excellent
 316 average predictive scores, while the MaxEnt models performed worst. According to the Boyce
 317 index individual performance, the RF models attained high levels of agreement between the
 318 presence dataset and grid cells with high HSI.



319

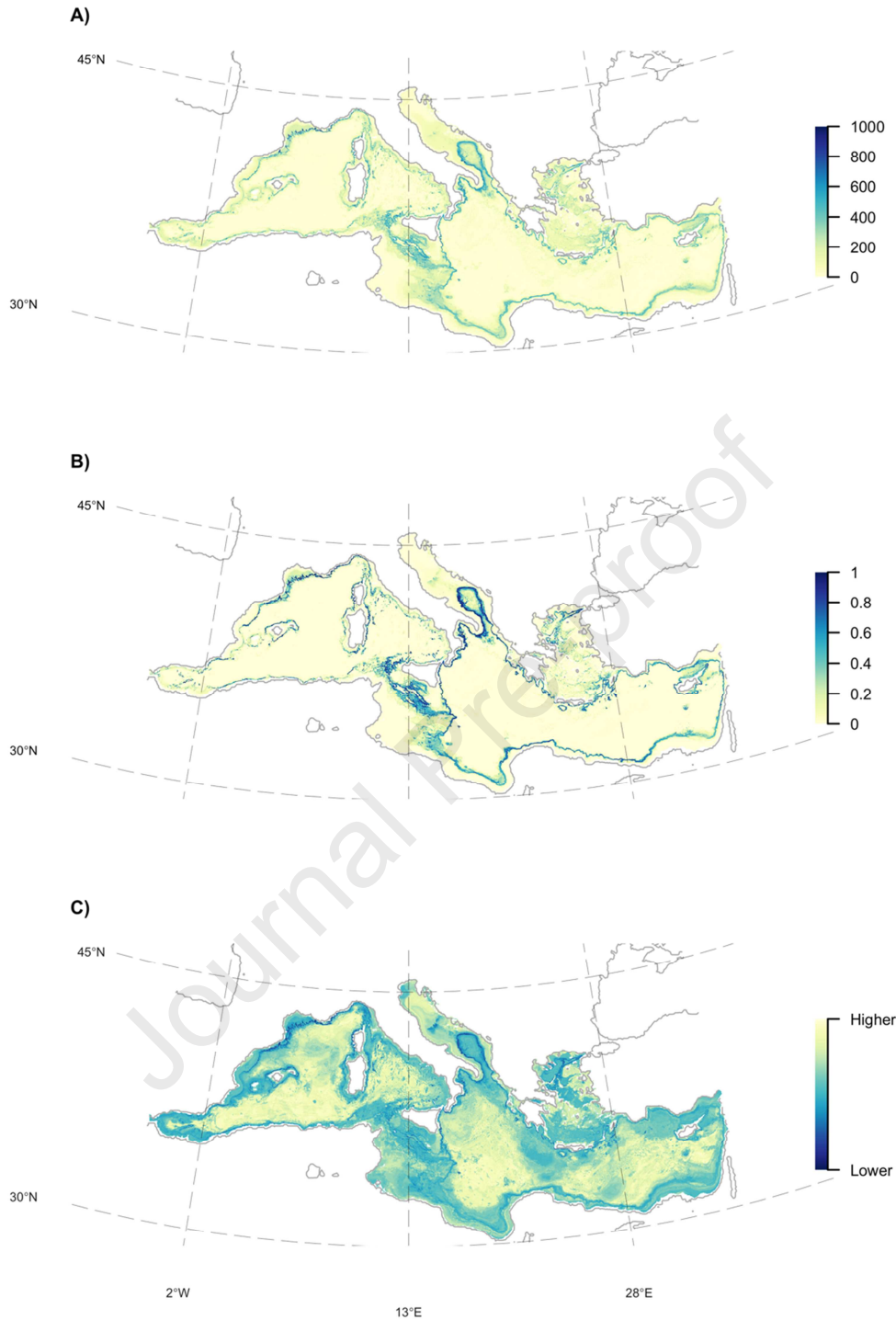
320 Fig. 5 - Performances of the models grouped by modelling algorithms (presence/pseudo-absence datasets and
 321 repetitions pooled) according to ROC, TSS and Boyce evaluation scores. The models' scores above the
 322 threshold indicated by the dashed lines are considered highly accurate. The average scores of single models are
 323 indicated by the white dots ($n = 100$). Black dots are the scores for the ensemble model.

324 The ensemble model forecast was built from the consensus of 198 out of the 300 simulated
 325 models, selected according to the defined TSS threshold (0.8). For the three metrics, the scores
 326 of the ensemble model were higher than the average scores of the single models indicating that
 327 it out-performed the estimation from the single algorithms.

328 3.3 Seascape suitability

329 The highest HSI values were found mainly along the upper slope of the Mediterranean margins,
 330 in the Western region (e.g., canyons in the Gulf of Lion), in the Central region of the
 331 Mediterranean Sea off the Island of Malta, and in the North of the Ionian Sea (deep-water coral
 332 provinces of Santa Maria di Leuca) and in the South Adriatic Sea (Fig. 6A). The HSI reached
 333 values close to zero in shallower (e.g., North Adriatic, and Tunisian and Libyan continental
 334 shelves) and abyssal depths.

335 The result of the committee averaging model (Fig. 6B) indicates high reliability (agreement
 336 between the presence/absence binary transformation of the single models' prediction) of the
 337 ensemble forecast for the most suitable and most unsuitable areas and low reliability (values
 338 around 0.5) overall for the upper slope of the Central and Southeastern Mediterranean regions.
 339 The coefficient of variance (Fig. 6C) returned overall a low uncertainty of the ensemble forecast
 340 along the upper slope of the Mediterranean margins and higher uncertainty for the abyssal areas
 341 and parts of the Northern Adriatic Sea.

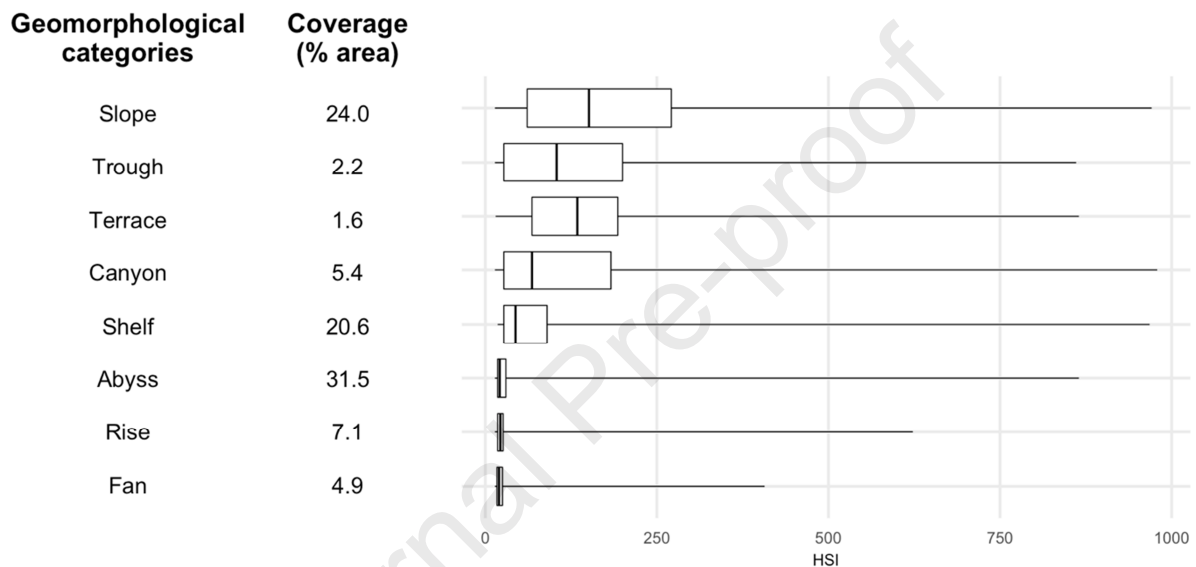


342

343 Fig. 6 - (A) Ensemble model based on the mean probabilities of the selected models and expressed as HSI
 344 (ranging from 0 to 1000, representing the least and the most suitable areas, respectively). (B) Map of the
 345 committee averaging score; this map offers a measure of reliability of the ensemble model (values close to 1 or 0
 346 indicate a good agreement among the single models' predictions regarding the potential presence or absence,
 347 respectively; values around 0.5 mean that the estimates of the models are evenly distributed by 0 and 1 values).
 348 (C) The coefficient of variance (i.e., standard deviation/mean) of the probabilities estimated for the selected
 349 models is also a measure of uncertainty: dark colours correspond to better predictions, while lighter colours mean
 350 that prediction uncertainty is higher.

351 Among the 15 geomorphologic features identified by Harris *et al.* (2014) in the Mediterranean
 352 Sea, ridges, shelf valleys, trenches, seamounts, guyots, bridges and sills represent individually

353 less than 1% of the seascape area (0.9, 0.9, 0.4, 0.3, 0.1, 0.01, <0.01%, respectively). The
 354 continental slopes and submarine canyons are, regarding the area covered, the two most
 355 relevant features with high HSI values estimated by our model (Fig. 7); together with troughs and
 356 terraces, they cover 33.2% of the Mediterranean seascape. The variation of the HSI estimates
 357 within each category was large, indicating a highly heterogeneous environment, and the limits of
 358 the third quartile remained below 287 for all categories. The geomorphologic categories showing
 359 the highest proportions of low suitability habitats (in all cases the third quartile showed HSI
 360 scores lower than 90) were the abyssal areas, continental shelves and rise, and submarine fans,
 361 in total accounting for 64.1% of the Mediterranean seascape.



362

363 Fig. 7 - Classification of seascape suitability of the geomorphologic feature categories (Harris et al., 2014)
 364 present along the Mediterranean Sea by decreasing order of the 3rd quartile. The lines indicate the HSI value
 365 ranges and the boxplots show the 1st quartile, the median and the 3rd quartile. The coverage percentages were
 366 given by the area of the shape of the polygons that defined the individual features in Harris et al. (2014).
 367 Features with an area lower than 1% were omitted.

368 A total of 898 MPAs, mostly encompassing coastal and shelf depths, confer some legal
 369 protection within the modelling region. From these MPAs, a clear majority allows multiple uses,
 370 and only 6.46%, covering a total area of 9863 km² ca. of 0.4% of the Mediterranean Sea area,
 371 have restriction to some type of fisheries or are no-take zones (Supplementary Fig. S2). Note
 372 that these values exclude the vast bottom trawl closure area, the largest non-fishing area in the
 373 Mediterranean Sea, covering depths greater than 1000 m, as well as the Shark and Cetacean
 374 Habitat Protected Areas and the Marine Mammal Sanctuary where the allowed fishing activities
 375 do not have relevant impacts on the seabed. The analysis of the overlap between the seascape
 376 suitability and Mediterranean MPAs showed that the vast majority of the areas with highest HSI
 377 values were not covered by any MPA (Supplementary Fig. S2). The few exceptions were the
 378 deepest areas located in the South of Italy, the Central Mediterranean region off the Island of
 379 Malta and the area around the Island of Crete which was covered by the bottom trawl closure.

380 4 Discussion

381 The output of a presence-only model is an estimation of the species environmental preferences
382 (Guillera-Arroita et al., 2015) and can be interpreted as a measure of habitat suitability for the
383 species occurrence. Species respond differently to a large variety of processes and
384 environmental constraints at local, regional and global scales. Hence, the analysis of the
385 organisms' distribution should take into consideration different levels of the environment spatial
386 hierarchy (Mackey and Lindenmayer, 2001). Our aim was not to provide a fine-scale assessment
387 of the Mediterranean seascape suitability for *L. pertusa*, for which the spatial resolution of the
388 ensemble model is not adequate. Instead, we present a continuous assessment of the
389 environmental conditions, compare the model results with the empirical knowledge on the
390 Mediterranean distribution of *L. pertusa* and provide relevant information to identify focal areas
391 for future efforts using higher resolution models currently only applicable at local scales. To our
392 best knowledge, this work is the first mesoscale (seascape level) estimation of the habitat
393 suitability for *L. pertusa* that encompasses the whole Mediterranean Sea using an ensemble
394 ENM with a multi-algorithm approach, providing both the prediction of seascape suitability and a
395 measure of uncertainty of the forecast.

396 4.1 A challenging ecological niche

397 The concept of ecological niche is central for the ENM approach, and the quality of the forecast
398 can be partly inferred from the response curves and their ecological plausibility. Despite some
399 variations between algorithms the bathymetry, bathymetric slope and pH showed the highest
400 contributions to the forecasts. Bathymetry and bathymetric slope are frequently selected as
401 relevant predictors to estimate the seascape suitability for *L. pertusa* (e.g., Barbosa et al., 2019;
402 Rengstorf et al., 2013; Ross and Howell, 2013). Similarly, for the pH, predictors related to ocean
403 acidification and the calcification of the corals' skeleton (e.g., aragonite saturation state – Ω_{ARAG})
404 are also among the variables with higher contribution in ENM studies focusing in *L. pertusa* (e.g.,
405 Davies and Guinotte, 2011; Morato et al., 2020). The limited availability of modern-day
406 observation data for the Mediterranean Sea regarding the carbonate chemistry hampers the
407 development of accurate chemistry models for the region. For this reason, we opted for not
408 including the Ω_{ARAG} in our ENM study. Notwithstanding, *in situ* data indicates that the
409 Mediterranean seawater is likely to remain supersaturated in the future (Fajar et al., 2015);
410 therefore, the Ω_{ARAG} may not be a major limiting factor for the *L. pertusa* distribution in the
411 Mediterranean Sea as it might be for other regions owing to the shallowing of the aragonite
412 saturation horizon (Lunden et al., 2013). In fact, the optimal bathymetric range estimated by our
413 model (Fig. 3) and the currently known distribution of the species in the region coincide with
414 depths considerably shallower than 2500 m (Fig. 2) for which seawater remains supersaturated
415 (Fajar et al., 2015; Schneider et al., 2007). Our results also agree with Davies and Guinotte
416 (2011) that the species distribution coincide mostly with areas with low concentrations of

417 nutrients and limited organic inputs. A strong link between CWC occurrence and the
418 hydrodynamic regime has often been reported (e.g., Rengstorf et al., 2014) but our results
419 indicate current velocity as one of the predictors contributing less to the model predictions. This
420 result can be partially explained by the relatively coarse resolution of our model that is insufficient
421 to represent the fine-scale local hydrodynamics and its complex interaction with topography,
422 probably underestimating the actual influence of this predictor on the species fine-scale spatial
423 distribution (Davies and Guinotte, 2011; Rengstorf et al., 2014). Salinity and dissolved oxygen
424 concentration were classified as relevant environmental predictors in previous ENM studies with
425 *L. pertusa* (e.g., Barbosa et al., 2019; Davies and Guinotte, 2011). In our study, these two
426 variables were however among the ones with lower contribution for the models' prediction. This
427 result may be related to the low spatial variability close to the seabed of these predictors in the
428 Mediterranean Sea (Supplementary Fig. S3). Surrogates of terrain variables derived from
429 bathymetry such as rugosity are also widely recognised as important proxies for habitat suitability
430 for CWC in local high-resolution models (e.g., Lo Iacono et al (2018)). However, we intentionally
431 excluded these variables because terrain attributes are highly scale-dependent and their
432 computation at coarse resolutions results in significant differences between the derived data and
433 the local characteristics (Rengstorf et al., 2012).

434 The distribution of living CWC in the Mediterranean Sea has been historically considered as
435 restricted, partly owing to the near homoeothermic conditions (12.7-14.5 °C, Delibrias and
436 Taviani, 1985). Our results show that in the Mediterranean Sea, *L. pertusa* lives at temperature
437 and salinity values (T: 13-14 °C; S: 38.1-38.8) that may be close to the upper limit of the species
438 tolerance. In fact, these values are considerably higher than the ones found in areas of the
439 northeast Atlantic Ocean with thriving *L. pertusa* reefs (T<10 °C, S< 35.6, Dullo et al., 2008).
440 Studies on the physiological response of *L. pertusa* to temperature variations revealed that
441 significant effects are observed on the calcification rate, despite the species capacity for thermal
442 adaptation (Naumann et al., 2014). Although *L. pertusa* shows some biogeographic physiological
443 plasticity to face environmental changes (Georgian et al., 2016), the populations in the
444 Mediterranean Sea may be already subjected to the limits of their physiological tolerance, as
445 already assumed by other authors (Freiwald et al., 2009; Maier et al., 2009).

446 The species distribution is also determined by the seawater chemistry that constraints the
447 calcification of the carbonate skeleton (Maier et al., 2009). Our model suggests a considerable
448 decrease of the seascape suitability for *L. pertusa* with pH reduction. Lowering pH values by
449 0.15-0.3 units in laboratory comparing to present North Atlantic Ocean conditions resulted in a
450 reduction of the calcification rate of 30-56% (Maier et al., 2009). The Mediterranean Sea shows a
451 westward trend of decreasing pH (Álvarez et al., 2014) and, despite the high buffering capacity of
452 the Mediterranean Sea (Schneider et al., 2007) this trend may be accentuated by further
453 accumulation of carbon from anthropogenic origin in the intermediate and deep waters (Fajar et
454 al., 2015). Therefore, the synergies of multiple stressors, especially in the current scenario of

455 global change, is expected to accentuate the already challenging environmental setting for the
456 species occurrence in the Mediterranean Sea.

457 4.2 Performance, predictive capacity and limitation of the ENM models

458 The good performance scores of the single models were surpassed by the ensemble model
459 scores in all metrics, strengthening our confidence in its predictive capacity. The estimates of the
460 committee averaging and coefficient of variance, indicating overall low uncertainty levels for the
461 forecast of the ensemble model further support the advantages of using this modelling approach.
462 The projection of the ensemble model over the Mediterranean Sea (Fig. 6A) encompasses areas
463 of medium to high HSI scores located along the upper slope along the Gulf of Lion and Central
464 Mediterranean region (i.e., around Corsica and Sardinia, off Malta and south of the Adriatic Sea).
465 The lowest HSI values cover vast areas including the continental shelves (<100 m depth) and the
466 deepest regions (>1500 m).

467 ENMs are scale-dependent, and predictions are overestimated for larger grid cells (Seo et al.,
468 2009); hence ground-truthing surveys are always required. Moreover, regardless of their
469 performance, ENMs commonly overestimate the species potential distributions since they
470 assume that their occurrence is largely influenced by the ecological niche, ignoring other
471 important drivers for species prevalence (Georgian et al., 2014). A species may be absent in
472 areas with suitable conditions owing to biotic interactions, oceanographic barriers (e.g., water
473 column stratification, prevailing currents) and other complex ecological mechanisms preventing
474 dispersal and/or colonization (Rogers, 2003). Moreover, ENM predictions are always coupled
475 with a certain level of uncertainty associated to the data characteristics (i.e., quality and quantity)
476 and to the methodological decisions made during the modelling process. Nevertheless, the
477 influence of various limitations on the models' forecasts are difficult to quantify. Among the main
478 sources of uncertainty affecting deep-sea ENM are the limitations in the occurrence datasets
479 which, in the case of *L. pertusa*, derive, at least partly, from an insufficient coverage by surveys
480 targeting CWC in the Mediterranean Sea. In the Mediterranean Sea, field observations indicate
481 that *L. pertusa* is less common than in other oceans and has a more patchy distribution, often
482 occurring as isolated colonies (Howell et al., 2011; Orejas et al., 2009). The increasing number of
483 biological surveys in the Mediterranean Sea and the growing tendency to use remote sensing
484 and underwater technologies in oceanographic cruises, is likely to increase the number of coral
485 areas detected in this region (Taviani et al., 2017). Recent efforts to catalogue coral occurrences
486 in the Mediterranean Sea (Chimienti et al., 2019; Taviani et al., 2019a) highlighted the existence
487 of an "almost uninterrupted, albeit patchy, belt of CWC sites" along the south-western Adriatic
488 margin (Angeletti et al., 2014) and a coral reef of considerable size was observed in the Lacaze-
489 Duthiers submarine canyon (Gori et al., 2013). These and other well-known CWC areas were
490 scored with high HSI by our model: the Santa Maria di Leuca coral province (e.g., Tursi *et al.*
491 (2004)), the South Adriatic (e.g., Freiwald *et al.* (2009), Angeletti *et al.* (2014), South of the Island

492 of Malta (e.g., Maier *et al.* (2012), the Melilla CWC Province (Lo-Iacono *et al.*, 2014), and several
493 submarine canyons (e.g., the Cap de Creus (Orejas *et al.*, 2011) and Lacaze-Duthiers (Fabri *et al.*
494 *et al.*, 2014) in the Gulf of Lion, Nora (Taviani *et al.*, 2017) in the South of the Island of Sardinia,
495 Bari (Freiwald *et al.*, 2009) in the South Adriatic Sea). The number of occurrences used in our
496 models probably influenced the ENM forecasts. Hence, to improve the predictive capacity of our
497 model, we selected algorithms that show good performances with a small number of presences
498 (Hernandez *et al.*, 2006; Mi *et al.*, 2017; Wisz *et al.*, 2008). The more reliable predictions of the
499 models coincided with known living CWC provinces and surrounding areas. On the other hand,
500 in the eastern Mediterranean Sea, where many fossil CWC occurrences are reported but no
501 living colonies of *L. pertusa*, an almost continuous belt along the continental slope was classified
502 with intermediate HSI values. Hence, future modelling efforts updated with more species records
503 may improve the seascape suitability forecast for the region. Uncertainties in the models'
504 predictions may also derive from the spatiotemporal variability of the environmental predictors.
505 We applied an up-scaling process to improve the spatial resolution of the environmental data
506 extracted from the CMEMS ocean models. The interpolated variables were positive and
507 significantly correlated ($p < 0.001$, Supplementary Fig. S4-7) with the *in situ* collected data,
508 generally reflecting the patterns observed in the WOA data, both along the depth, longitude and
509 latitude gradients. These results attest to the accuracy of the interpolated layers and therefore
510 minimize the uncertainty on the models' predictions that can be derived from environmental data.

511 4.3 Mediterranean seascape suitability

512 Previous studies using predictive modelling at global and regional scales identified the
513 continental slopes (Davies and Guinotte, 2011) and geomorphologic features such as canyons
514 (Rengstorf *et al.*, 2013) as offering the most suitable conditions for *L. pertusa* occurrence. The
515 ranking of submarine canyons with some of the highest HSI scores in our ensemble model
516 confirms previous indications that, as a consequence of their complex topography and influence
517 on hydrodynamics, these geomorphologic features may be considered CWC hotspots (Orejas *et al.*
518 *et al.*, 2009; Van den Beld *et al.*, 2017). The high-energy environments and roughed topography
519 commonly associated with canyons can result in low sediment coverage and higher availability of
520 hard substrates for reef development (Sánchez *et al.*, 2014). Such conditions may also be
521 frequently found in escarpments and rocky outcrops on continental slopes. Seamounts (and
522 guyots) are also recognized as preferential areas for CWC development (Roberts *et al.*, 2009).
523 Despite the relatively coarse resolution of our model (230 x 230 m) and the low percentage
524 coverage occupied by seamounts in the Mediterranean Sea (Harris *et al.*, 2014), some areas
525 classified with higher HSI in regions such as the Alboran Sea (Fig. 6A), coincide with the location
526 of these features (Rovere and Würtz, 2015).

527 Apart from the ecological reasons mentioned above, species distributions can be constrained by
528 the type, intensity and frequency of anthropogenic disturbance. Human activities can lead to

529 local extinctions of vulnerable species from otherwise environmental suitable locations (Clark et
530 al., 2016). Many studies exposed severe impacts on CWC populations (Fabri et al., 2014;
531 Taviani et al., 2019a) that result from fishing activities, litter accumulation and waste disposal.
532 Conservation measures to mitigate some of these detrimental activities are implemented in
533 areas classified as Sensitive Habitats by the European Commission and/or marine Sites of
534 Community Importance (p-SCI) included in the Natura 2000 network (Madurell et al., 2013).
535 However, these examples correspond mainly to MPAs covering coastal and shelf regions and
536 therefore not effectively protecting *L. pertusa*. The bottom trawl closure area is a clear exception,
537 but despite its great importance and extent, the exclusion of fishing activities below the 1000 m
538 may only provide partial protection to *L. pertusa* since it barely overlaps with the deepest fringe
539 of the most suitable areas. Besides, locations classified with high HSI coincide with areas with
540 medium to high cumulative human impacts in Mediterranean ecosystems (Micheli et al., 2013).
541 Considering these issues, the conservation of *L. pertusa* habitat and the persistence of its
542 Mediterranean populations could be at risk with serious consequences for the biodiversity and
543 functioning of deep-sea ecosystems (particularly at the continental slopes). In this context,
544 canyons may have a supplementary conservation value acting as natural refuges for CWC
545 against some of the anthropogenic impacts (e.g., bottom trawling (Van den Beld et al., 2017),
546 particularly because the Mediterranean Sea is one of the world's regions where canyons are
547 more densely and closely spaced (Harris and Whiteway, 2011) occupying naturally delimited and
548 therefore potentially more manageable areas for conservation purposes.

549 4.4 Conclusion

550 Regardless of their limitations, ENMs are important to compile and interpret information on the
551 species ecology, provide insights on their potential distributions and are particularly relevant for
552 research on data-poor species (Morato et al., 2020; Vierod et al., 2014). Our seascape suitability
553 assessment broadens the perception of the Mediterranean potential distribution of *L. pertusa*,
554 and its ecological constraints, previously based on fragmented information from punctual
555 biological surveys and local modelling efforts. The results show that *L. pertusa* in the
556 Mediterranean Sea seems to be subjected to physiological stress due to the current
557 environmental conditions observed in the area. Despite eventual biogeographic plasticity in the
558 physiological response of *L. pertusa*, the resilience of the Mediterranean reefs may be
559 compromised by a further intensification of stressful conditions. This scenario is likely to occur
560 under the current climate change trend, increasing anthropogenic pressure and lack of adequate
561 protection of CWC habitats in the Mediterranean Sea. The mapping of the seascape
562 environmental suitability of *L. pertusa* may assist future research efforts, including further
563 modelling studies with higher resolution data on the areas identified as most suitable, the
564 development of action plans for their conservation and the investigation of the mechanisms
565 governing the persistence of *L. pertusa* reefs in the Mediterranean Sea.

566 **Acknowledgments**

567 The first author was funded by a PhD grant from Fundação para a Ciência e Tecnologia (FCT)
 568 (SFRH/BD/92433/2013). We are most grateful to Damien Georges for his valuable help in the
 569 modeling technical procedures, and to João Luís Oliveira Carvalho (DBIO-UA & CESAM) for his
 570 comments and suggestions to the manuscript. We would also like to acknowledge the technical
 571 support of Luís Carvalheiro with the ARGUS High-Performance Computing Cluster from the
 572 University of Aveiro. This study was partially funded by FCT/MCTES by the financial support to
 573 CESAM (UIDP/50017/2020+UIDB/50017/2020), through national funds.

574

575 **Author Contributions**

576 FM, JC and MC conceived the study; FM and MC analysed the results; FM, JC and MC wrote
 577 the manuscript. All authors reviewed the manuscript.

578 **Reference**

- 579 Aguirre-Gutiérrez, J., Carvalheiro, L.G., Polce, C., van Loon, E.E., Raes, N., Reemer, M., Biesmeijer,
 580 J.C., 2013. Fit-for-Purpose: Species Distribution Model Performance Depends on Evaluation
 581 Criteria – Dutch Hoverflies as a Case Study. *PLoS One* 8, e63708 EP –.
 582 doi:10.1371/journal.pone.0063708
- 583 Aiello-Lammens, M.E., Boria, R.A., Radosavljevic, A., Vilela, B., Anderson, R.P., 2015. spThin: an R
 584 package for spatial thinning of species occurrence records for use in ecological niche models.
 585 *Ecography* 38, 541–545. doi:10.1111/ecog.01132
- 586 Anderson, O.F., Guinotte, J.M., Rowden, A.A., Clark, M.R., Mormede, S., Davies, A.J., Bowden, D.A.,
 587 2016. Field validation of habitat suitability models for vulnerable marine ecosystems in the South
 588 Pacific Ocean: Implications for the use of broad-scale models in fisheries management. *Ocean*
 589 *Coast Manag* 120, 110–126. doi:10.1016/j.ocecoaman.2015.11.025
- 590 Anderson, R.P., Gonzalez, I., Jr, 2011. Species-specific tuning increases robustness to sampling bias
 591 in models of species distributions: An implementation with Maxent. *Ecol. Modell.* 222, 2796–
 592 2811. doi:10.1016/j.ecolmodel.2011.04.011
- 593 Angeletti, L., Taviani, M., Canese, S., Fogliani, F., Mastrototaro, F., Argnani, A., Trincardi, F., Bakran-
 594 Petricioli, T., Ceregato, A., Chimienti, G., Macic, V., Poliseo, A., 2014. New deep-water
 595 cnidarian sites in the southern Adriatic Sea. *Mediterr. Mar. Sci.* 15, 263–273.
 596 doi:10.12681/mms.558
- 597 Araújo, M.B., New, M., 2007. Ensemble forecasting of species distributions. *Trends Ecol. Evol.* 22,
 598 42–47. doi:10.1016/j.tree.2006.09.010
- 599 Assis, J., Tyberghein, L., Bosch, S., Verbruggen, H., Serrao, E.A., De Clerck, O., 2018. Bio-ORACLE
 600 v2.0: Extending marine data layers for bioclimatic modelling. *Glob. Ecol. Biogeogr.* 27, 277–284.
 601 doi:10.1111/geb.12693
- 602 Álvarez, M., Sanleon-Bartolome, H., Tanhua, T., Mintrop, L., Luchetta, A., Cantoni, C., Schroeder, K.,
 603 Civitarese, G., 2014. The CO₂ system in the Mediterranean Sea: a basin wide perspective.
 604 *Ocean Science* 10, 69–92. doi:10.5194/os-10-69-2014
- 605 Barbet-Massin, M., Jiguet, F., Albert, C.H., Thuiller, W., 2012. Selecting pseudo-absences for species
 606 distribution models: how, where and how many? *Methods Ecol. Evol.* 3, 327–338.
 607 doi:10.1111/j.2041-210X.2011.00172.x
- 608 Barbosa, R.V., Davies, A.J., Sumida, P.Y.G., 2019. Habitat suitability and environmental niche
 609 comparison of cold-water coral species along the Brazilian continental margin. *Deep Sea Res.*
 610 *Part I Oceanogr. Res. Pap.* 103147. doi:10.1016/j.dsr.2019.103147
- 611 Basher, Z., Bowden, D.A., Costello, M.J., 2014. Diversity and Distribution of Deep-Sea Shrimps in the
 612 Ross Sea Region of Antarctica. *PLoS One* 9, e103195. doi:10.1371/journal.pone.0103195

- 613 Boyce, M.S., Vernier, P.R., Nielsen, S.E., Schmiegelow, F.K.A., 2002. Evaluating resource selection
614 functions. *Ecol. Modell.* 157, 281–300. doi:10.1016/S0304-3800(02)00200-4
- 615 Buhl-Mortensen, L., Vanreusel, A., Gooday, A.J., Levin, L.A., Priede, I.G., Buhl-Mortensen, P.,
616 Gheerardyn, H., King, N.J., Raes, M., 2010. Biological structures as a source of habitat
617 heterogeneity and biodiversity on the deep ocean margins. *Marine Ecology* 31, 21–50.
618 doi:10.1111/j.1439-0485.2010.00359.x
- 619 Burgman, M.A., Lindenmayer, D.B., Elith, J., 2005. Managing Landscapes for Conservation Under
620 Uncertainty. *Ecology* 86, 2007–2017. doi:10.1890/04-0906
- 621 Capezzuto, F., Ancona, F., Carlucci, R., Carluccio, A., Cornacchia, L., Maiorano, P., Ricci, P., Sion,
622 L., Tursi, A., D'Onghia, G., 2018. Cold-water coral communities in the Central Mediterranean:
623 aspects on megafauna diversity, fishery resources and conservation perspectives. *Rend. Fis.*
624 *Acc. Lincei* 15, 1–9. doi:10.1007/s12210-018-0724-5
- 625 Carvalho, J., Santos, J.P.V., Torres, R.T., Santarém, F., Fonseca, C., 2017. Tree-Based Methods:
626 Concepts, Uses and Limitations under the Framework of Resource Selection Models.
627 doi:10.3808/jei.201600352
- 628 Chimienti, G., Bo, M., Mastrototaro, F., 2018. Know the distribution to assess the changes:
629 Mediterranean cold-water coral bioconstructions. *Rend. Fis. Acc. Lincei* 15, 1–6.
630 doi:10.1007/s12210-018-0718-3
- 631 Chimienti, G., Bo, M., Taviani, M., Mastrototaro, F., 2019. Occurrence and Biogeography of
632 Mediterranean Cold-Water Corals, in: Orejas, C., Jiménez, C. (Eds.), *Mediterranean Cold-Water*
633 *Corals: Past, Present and Future*. Springer International Publishing, Cham, pp. 213–243.
634 doi:10.1007/978-3-319-91608-8_19
- 635 Clark, M.R., Althaus, F., Schlacher, T.A., Williams, A., Bowden, D.A., Rowden, A.A., 2016. The
636 impacts of deep-sea fisheries on benthic communities: A review. *ICES J. Mar. Sci.* 73, i51–i69.
637 doi:10.1093/icesjms/fsv123
- 638 Corbera, G., Lo-Iacono, C., Gràcia, E., Grinyo, J., Pierdomenico, M., Huvenne, V., Aguilar, R., Gili, J.-
639 M., 2019. Ecological characterisation of a Mediterranean cold-water coral reef: Cabliers Coral
640 Mound Province (Alboran Sea, western Mediterranean). *Prog. Oceanogr.* 175, 245–262.
641 doi:10.1016/J.POCEAN.2019.04.010
- 642 D'Onghia, G., Calculli, C., Capezzuto, F., Carlucci, R., Carluccio, A., Grehan, A., Indennidate, A.,
643 Maiorano, P., Mastrototaro, F., Pollice, A., Russo, T., Savini, A., Sion, L., Tursi, A., 2017.
644 Anthropogenic impact in the Santa Maria di Leuca cold-water coral province (Mediterranean
645 Sea): Observations and conservation straits. *Deep Sea Res. Part II Top. Stud. Oceanogr.* 145,
646 87–101. doi:10.1016/j.dsr2.2016.02.012
- 647 Davies, A.J., Guinotte, J.M., 2011. Global habitat suitability for framework-forming cold-water corals.
648 *PLoS One* 6, e18483. doi:10.1371/journal.pone.0018483
- 649 Delibrias, G., Taviani, M., 1985. Dating the death of Mediterranean deep-sea scleractinian corals.
650 *Mar. Geol.* 62, 175–180. doi:10.1016/0025-3227(84)90062-8
- 651 Di Cola, V., Olivier, B., Blaise, P., T, B.F., Manuela, D., Christophe, R., Robin, E., Julien, P.,
652 Dorothea, P., Anne, D., Loic, P., G, M.R., Wim, H., Nicolas, S., Antoine, G., 2017. ecospat: an R
653 package to support spatial analyses and modeling of species niches and distributions. *Ecography*
654 40, 774–787. doi:10.1111/ecog.02671
- 655 Dullo, W.-C., Flögel, S., Rüggeberg, A., 2008. Cold-water coral growth in relation to the hydrography
656 of the Celtic and Nordic European continental margin. *Mar. Ecol. Prog. Ser.* 371, 165–176.
657 doi:10.3354/meps07623
- 658 EMODnet Bathymetry Consortium, 2016. EMODnet Digital Bathymetry (DTM).
659 doi:http://doi.org/10.12770/c7b53704-999d-4721-b1a3-04ec60c87238
- 660 Fabri, M.-C., Bargain, A., Pairaud, I., Pedel, L., Taupier-Letage, I., 2017. Cold-water coral ecosystems
661 in Cassidaigne Canyon: An assessment of their environmental living conditions. *Deep Sea Res.*
662 *Part II Top. Stud. Oceanogr.* 137, 436–453. doi:10.1016/j.dsr2.2016.06.006
- 663 Fabri, M.-C., Pedel, L., Beuck, L., Galgani, F., Hebbeln, D., Hebbeln, D., Freiwald, A., 2014.
664 Megafauna of vulnerable marine ecosystems in French mediterranean submarine canyons:
665 Spatial distribution and anthropogenic impacts. *Deep Sea Res. Part II Top. Stud. Oceanogr.* 104,
666 184–207. doi:10.1016/j.dsr2.2013.06.016
- 667 Fajar, N.M., García-Ibáñez, M.I., SanLeón-Bartolomé, H., Álvarez, M., Pérez, F.F., 2015.
668 Spectrophotometric Measurements of the Carbonate Ion Concentration: Aragonite Saturation
669 States in the Mediterranean Sea and Atlantic Ocean. *Environ Sci Technol* 49, 11679–11687.
670 doi:10.1021/acs.est.5b03033

- 671 Fink, H.G., Wienberg, C., De Pol-Holz, R., Hebbeln, D., 2015. Spatio-temporal distribution patterns of
 672 Mediterranean cold-water corals (*Lophelia pertusa* and *Madrepora oculata*) during the past
 673 14,000 years. *Deep Sea Res. Part I Oceanog. Res. Papers* 103, 37–48. doi:10.1594/PANGAEA
 674 Freiwald, A., Beuck, L., Rüggeberg, A., Taviani, M., Hebbeln, D., Hebbeln, D., 2009. The white coral
 675 community in the Central Mediterranean Sea revealed by ROV surveys. *Oceanography* 22, 58–
 676 74. doi:10.5670/oceanog.2009.06
 677 [dataset] Freiwald, A., Rogers, A.D., Hall-Spencer, J., Guinotte, J.M., Davies, A.J., Yesson, C., Martin,
 678 C.S., Weatherdon, L., 2017. Global distribution of cold-water corals (version 3.0). Second update
 679 to the dataset in Freiwald et al (2004) by UNEP-WCMC, in collaboration with Andre Freiwald and
 680 John Guinotte.
 681 Garcia, E.H., Locarnini, R.A., Boyer, T.P., Antonov, J.I., Mishonov, A.V., Baranova, O.K., Zweng,
 682 M.M., Reagan, J.R., Johnson, D.R., 2013. World ocean atlas 2013. Volume 3, Dissolved oxygen,
 683 apparent oxygen utilization, and oxygen saturation. NOAA Atlas NESDIS 75.
 684 Garcia, H.E., Locarnini, R.A., Boyer, T.P., Antonov, J.I., Baranova, O.K., Zweng, M.M., Reagan, J.R.,
 685 Johnson, D.R., 2013. World ocean atlas 2013. Volume 4, Dissolved inorganic nutrients
 686 (phosphate, nitrate, silicate). NOAA Atlas NESDIS 76.
 687 Georgian, S.E., Dupont, S., Kurman, M., Butler, A., Strömberg, S.M., Larsson, A.I., Cordes, E.E.,
 688 2016. Biogeographic variability in the physiological response of the cold-water coral *Lophelia*
 689 *pertusa* to ocean acidification. *Mar. Ecol.* 37, 1345–1359. doi:10.1111/maec.12373
 690 Georgian, S.E., Shedd, W., Cordes, E.E., 2014. High-resolution ecological niche modelling
 691 of the cold-water coral *Lophelia pertusa* in the Gulf of Mexico. *Mar. Ecol. Prog. Ser.* 506, 145–
 692 161. doi:10.3354/meps10816
 693 Giovanni Chimienti, F.M., D'Onghia, G., 2019. Mesophotic and Deep-Sea Vulnerable Coral Habitats
 694 of the Mediterranean Sea: Overview and Conservation Perspectives, in: *Advances in the Studies*
 695 *of the Benthic Zone*. IntechOpen. doi:10.5772/intechopen.90024
 696 Giusti, M., Canese, S., Fourt, M., Bo, M., Innocenti, C., Goujard, A., Daniel, B., Angeletti, L., Taviani,
 697 M., Aquilina, L., Tunesi, L., 2019. Coral forests and Derelict Fishing Gears in submarine canyon
 698 systems of the Ligurian Sea. *Prog Oceanogr* 178, 102186. doi:10.1016/j.pocean.2019.102186
 699 González-Irusta, J.M., González-Porto, M., Sarralde, R., Arrese, B., Almón, B., Martín-Sosa, P., 2015.
 700 Comparing species distribution models: a case study of four deep sea urchin species.
 701 *Hydrobiologia* 745, 43–57.
 702 Gori, A., Orejas, C., Madurell, T., Bramanti, L., Martins, M., Quintanilla, E., Marti-Puig, P., Lo-Iacono,
 703 C., Puig, P., Requena, S., Greenacre, M., Gili, J.M., 2013. Bathymetrical distribution and size
 704 structure of cold-water coral populations in the Cap de Creus and Lacaze-Duthiers canyons
 705 (northwestern Mediterranean). *Biogeosciences* 10, 2049–2060. doi:10.5194/bg-10-2049-2013
 706 Guillera-Aroita, G., Lahoz-Monfort, J.J., Elith, J., Gordon, A., Kujala, H., Lentini, P.E., McCarthy,
 707 M.A., Tingley, R., Wintle, B.A., 2015. Is my species distribution model fit for purpose? Matching
 708 data and models to applications. *Glob. Ecol. Biogeogr.* 24, 276–292. doi:10.1111/geb.12268
 709 Harris, P.T., Macmillan-Lawler, M., Rupp, J., Baker, E.K., 2014. Geomorphology of the oceans. *Mar.*
 710 *Geol.* 352, 4–24. doi:10.1016/j.margeo.2014.01.011
 711 Harris, P.T., Whiteway, T., 2011. Global distribution of large submarine canyons: Geomorphic
 712 differences between active and passive continental margins. *Mar. Geol.* 285, 69–86.
 713 doi:10.1016/j.margeo.2011.05.008
 714 Hennige, S.J., Wicks, L.C., Kamenos, N.A., Bakker, D.C.E., Findlay, H.S., Dumousseaud, C.,
 715 Roberts, J.M., 2014. Short-term metabolic and growth responses of the cold-water coral *Lophelia*
 716 *pertusa* to ocean acidification. *Deep Sea Res. Part II Top. Stud. Oceanogr.* 99, 27–35.
 717 doi:10.1016/j.dsr2.2013.07.005
 718 Hernandez, P.A., Graham, C.H., Master, L.L., Albert, D.L., 2006. The effect of sample size and
 719 species characteristics on performance of different species distribution modeling methods.
 720 *Ecography* 29, 773–785. doi:10.1111/j.0906-7590.2006.04700.x
 721 Hirzel, A.H., Le Lay, G., Helfer, V., Randin, C., Guisan, A., 2006. Evaluating the ability of habitat
 722 suitability models to predict species presences. *Ecol. Modell.* 199, 142–152.
 723 doi:10.1016/j.ecolmodel.2006.05.017
 724 Hofstra, N., Haylock, M., New, M., Jones, P., Frei, C., 2008. Comparison of six methods for the
 725 interpolation of daily, European climate data. *Journal of Geophysical Research: Atmospheres*
 726 113. doi:10.1029/2008JD010100
 727 Howell, K., Holt, R., Endrino, I.P., Stewart, H., 2011. When the species is also a habitat: Comparing
 728 the predictively modelled distributions of *Lophelia pertusa* and the reef habitat it forms. *Biol.*
 729 *Conserv.* 144, 2656–2665. doi:10.1016/j.biocon.2011.07.025

- 730 Linley, T.D., Lavaleye, M., Maiorano, P., Bergman, M., Capezzuto, F., Cousins, N.J., D'Onghia, G.,
731 Duineveld, G., Shields, M.A., Sion, L., Tursi, A., Priede, I.G., 2017. Effects of cold water corals
732 on fish diversity and density (European continental margin: Arctic, NE Atlantic and Mediterranean
733 Sea): Data from three baited lander systems. *Deep Sea Res. Part II Top. Stud. Oceanogr.* 145,
734 8–21. doi:10.1016/j.dsr2.2015.12.003
- 735 Lo-lacono, C., Gràcia, E., Ranero, C.R., Emelianov, M., Huvenne, V., Bartolomé, R., Booth-Rea, G.,
736 Prades, J., 2014. The West Melilla cold water coral mounds, Eastern Alboran Sea: Morphological
737 characterization and environmental context. *Deep Sea Res. Part II Top. Stud. Oceanogr.* 99,
738 316–326. doi:10.1016/j.dsr2.2013.07.006
- 739 Lo-lacono, C., Robert, K., Gonzalez-Villanueva, R., Gori, A., Gili, J.-M., Orejas, C., 2018. Predicting
740 cold-water coral distribution in the Cap de Creus Canyon (NW Mediterranean): Implications for
741 marine conservation planning. *Prog. Oceanogr.* 169, 169–180. doi:10.1016/j.pocean.2018.02.012
- 742 Lobo, J.M., Valverde, A.J., Real, R., 2008. AUC: a misleading measure of the performance of
743 predictive distribution models. *Glob. Ecol. Biogeogr.* 17, 145–151. doi:10.1111/j.1466-
744 8238.2007.00358.x
- 745 Locarnini, R.A., Mishonov, A.V., Antonov, J.I., Boyer, T.P., Garcia, H.E., Baranova, O.K., Zweng,
746 M.M., Paver, C.R., Reagan, J.R., Johnson, D.R., Hamilton, M., Seidov, D., 2013. World Ocean
747 Atlas 2013, Volume 1: Temperature. NOAA Atlas NESDIS 73.
- 748 Lunden, J.J., Georgian, S.E., Cordes, E.E., 2013. Aragonite saturation states at cold-water coral reefs
749 structured by *Lophelia pertusa* in the northern Gulf of Mexico. *Limnology and Oceanography* 58,
750 354–362. doi:10.4319/lo.2013.58.1.0354
- 751 Mackey, B.G., Lindenmayer, D.B., 2001. Towards a hierarchical framework for modelling the spatial
752 distribution of animals. *J. Biogeogr.* 28, 1147–1166. doi:10.1046/j.1365-2699.2001.00626.x
- 753 Madurell, T., Zabala, M., Dominguez-Carrio, C., Gili, J.M., 2013. Bryozoan faunal composition and
754 community structure from the continental shelf off Cap de Creus (Northwestern Mediterranean). *J*
755 *Sea Res* 83, 123–136. doi:10.1016/j.seares.2013.04.013
- 756 Maier, C., Hegeman, J., Weinbauer, M.G., Gattuso, J.P., 2009. Calcification of the cold-water coral
757 *Lophelia pertusa* under ambient and reduced pH. *Biogeosciences* 6, 1671–1680. doi:10.5194/bg-
758 6-1671-2009
- 759 Maier, C., Watremez, P., Taviani, M., Weinbauer, M.G., Gattuso, J.P., 2012. Calcification rates and
760 the effect of ocean acidification on Mediterranean cold-water corals. *Proc. Biol. Sci.* 279, 1716–
761 1723. doi:10.1098/rspb.2011.1763
- 762 Mi, C., Huettmann, F., Guo, Y., Han, X., Wen, L., 2017. Why choose Random Forest to predict rare
763 species distribution with few samples in large undersampled areas? Three Asian crane species
764 models provide supporting evidence. *PeerJ* 5, e2849. doi:10.7717/peerj.2849
- 765 Micheli, F., Halpern, B.S., Walbridge, S., Ciriaco, S., Ferretti, F., Fraschetti, S., Lewison, R.L.,
766 Nykjaer, L., Rosenberg, A.A., 2013. Cumulative human impacts on Mediterranean and Black Sea
767 marine ecosystems: Assessing current pressures and opportunities. *PLoS One* 8, e79889.
768 doi:10.1371/journal.pone.0079889
- 769 Miller, J.A., 2010. Species distribution modeling. *Geogr. Compass.* 4, 490–509. doi:10.1111/j.1749-
770 8198.2010.00351.x
- 771 Morato, T., Irusta, J.M.G., Carrió, C.D., Wei, C.-L., Davies, A.J., Sweetman, A.K., Taranto, G.H.,
772 Beazley, L., Alegre, A.G., Grehan, A., Laffargue, P., Murillo, F.J., Sacau, M., Vaz, S.,
773 Kenchington, E., Haond, S.A., Callery, O., Chimienti, G., Cordes, E., Egilsdóttir, H., Freiwald, A.,
774 Gasbarro, R., Zárate, C.G., Gianni, M., Gilkinson, K., Hayes, V.E.W., Hebbeln, D., Hedges, K.,
775 Henry, L.-A.A., Johnson, D., Alonso, M.K., Lirette, C., Mastrototaro, F., Menot, L., Molodtsova, T.,
776 Muñoz, P.D., Orejas, C., Pennino, M.G., Puerta, P., Ragnarsson, S.Á., Sánchez, B.R., Rice, J.,
777 Rivera, J., Roberts, J.M., Ross, S.W., Rueda, J.L., Sampaio, Í., Snelgrove, P., Stirling, D., Treble,
778 M.A., Urra, J., Vad, J., van Oevelen, D., Watling, Les, Walkusz, W., Wienberg, C., Woillez, M.,
779 Levin, L.A., Silva, M.C., 2020. Climate-induced changes in the suitable habitat of cold water
780 corals and commercially important deep sea fishes in the North Atlantic. *Global Change Biology*
781 26, 2181–2202. doi:10.1111/gcb.14996
- 782 Movilla, J., Orejas, C., Calvo, E., Gori, A., Lopez-Sanz, A., Grinyo, J., Dominguez-Carrio, C., Pelejero,
783 C., 2014. Differential response of two Mediterranean cold-water coral species to ocean
784 acidification. *Coral Reefs* 33, 675–686. doi:10.1007/s00338-014-1159-9
- 785 Naumann, M.S., Orejas, C., Ferrier-Pages, C., 2014. Species-specific physiological response by the
786 cold-water corals *Lophelia pertusa* and *Madrepora oculata* to variations within their natural
787 temperature range. *Deep Sea Res. Part II Top. Stud. Oceanogr.* 99, 36–41.
788 doi:10.1016/j.dsr2.2013.05.025

- 789 Omri, A., Asaf, T., Ronen, K., 2006. Assessing the accuracy of species distribution models:
790 prevalence, kappa and the true skill statistic (TSS). *J. Appl. Ecol.* 43, 1223–1232.
791 doi:10.1111/j.1365-2664.2006.01214.x
- 792 Orejas, C., Ferrier-Pages, C., Reynaud, S., Gori, A., Beraud, E., Tsounis, G., Allemand, D., Gili, J.M.,
793 2011. Long-term growth rates of four Mediterranean cold-water coral species maintained in
794 aquaria. *Mar. Ecol. Prog. Ser.* 429, 57–65. doi:10.3354/meps09104
- 795 Orejas, C., Gori, A., Lo-Iacono, C., Puig, P., Gili, J.M., Dale, M.R.T., 2009. Cold-water corals in the
796 Cap de Creus canyon, northwestern Mediterranean: spatial distribution, density and
797 anthropogenic impact. *Mar. Ecol. Prog. Ser.* 397, 37–51. doi:10.3354/meps08314
- 798 Pearce, J.L., Ferrier, S., 2000. Evaluating the predictive performance of habitat models developed
799 using logistic regression. *Ecol. Modell.* 133, 225–245. doi:10.1016/S0304-3800(00)00322-7
- 800 Peterson, A.T., Papeş, M., Soberón, J., 2015. Mechanistic and Correlative Models of Ecological
801 Niches. *European Journal of Ecology* 1, 28–38. doi:10.1515/eje-2015-0014
- 802 Philips, S.J., Miroslav, D., 2008. Modeling of species distributions with Maxent: new extensions and a
803 comprehensive evaluation. *Ecography* 31, 161–175. doi:10.1111/j.0906-7590.2008.5203.x
- 804 R Core Team, 2016. R: A Language and Environment for Statistical Computing. R Foundation for
805 Statistical Computing.
- 806 Reiss, H., Birchenough, S., Borja, A., Buhl-Mortensen, L., Craeymeersch, J., Dannheim, J., Darr, A.,
807 Galparsoro, I., Gogina, M., Neumann, H., Populus, J., Rengstorf, A.M., Valle, M., Van Hoey, G.,
808 Zettler, M.L., Degraer, S., 2015. Benthos distribution modelling and its relevance for marine
809 ecosystem management. *ICES J. Mar. Sci.* 72, 297–315. doi:10.1093/icesjms/fsu107
- 810 Rengstorf, A.M., Grehan, A., Yesson, C., Brown, C., 2012. Towards High-Resolution Habitat
811 Suitability Modeling of Vulnerable Marine Ecosystems in the Deep-Sea: Resolving Terrain
812 Attribute Dependencies. *Mar. Geod.* 35, 343–361. doi:10.1080/01490419.2012.699020
- 813 Rengstorf, A.M., Mohn, C., Brown, C., Wisz, M.S., Grehan, A.J., 2014. Predicting the distribution of
814 deep-sea vulnerable marine ecosystems using high-resolution data: Considerations and novel
815 approaches. *Deep Sea Res. Part I Oceanogr. Res. Pap.* 93, 72–82.
816 doi:10.1016/j.dsr.2014.07.007
- 817 Rengstorf, A.M., Yesson, C., Brown, C., Grehan, A.J., Crame, A., 2013. High-resolution habitat
818 suitability modelling can improve conservation of vulnerable marine ecosystems in the deep sea.
819 *J. Biogeogr.* 40, 1702–1714. doi:10.1111/jbi.12123
- 820 Roberts, J.M., Murray, F., Anagnostou, E., Hennige, S., Gori, A., Henry, L.-A.A., Fox, A.D., Kamenos,
821 N., Foster, G.L., 2016. Cold-Water Corals in an Era of Rapid Global Change: Are These the
822 Deep Ocean's Most Vulnerable Ecosystems?, in: Goffredo, S., Dubinsky, Z. (Eds.), *The Cnidaria,*
823 *Past, Present and Future: the World of Medusa and Her Sisters.* Springer International
824 Publishing, Cham, pp. 593–606. doi:10.1007/978-3-319-31305-4_36
- 825 Roberts, J.M., Wheeler, A., Freiwald, A., Cairns, S., 2009. Cold-Water Corals, Cold-Water Corals,
826 The Biology and Geology of Deep-Sea Coral Habitats. Cambridge University Press, Cambridge.
827 doi:10.1017/CBO9780511581588.003
- 828 Rogers, A.D., 2003. Molecular Ecology and Evolution of Slope Species, in: *Ocean Margin Systems.*
829 Springer Berlin Heidelberg, Berlin, Heidelberg, pp. 323–337. doi:10.1007/978-3-662-05127-6_20
- 830 Rogers, A.D., 1999. The Biology of *Lophelia pertusa* (Linnaeus 1758) and Other Deep-Water Reef-
831 Forming Corals and Impacts from Human Activities. *Int. Rev. Hydrobiol.* 84, 315–406.
- 832 Ross, R.E., Howell, K., 2013. Use of predictive habitat modelling to assess the distribution and extent
833 of the current protection of “listed” deep-sea habitats. *Divers. Distrib.* 19, 433–445.
834 doi:10.1111/ddi.12010
- 835 Rovere, M., Würtz, M., 2015. Atlas of the Mediterranean seamounts and seamount-like structures.
836 IUCN, Malaga. doi:https://doi.org/10.2305/IUCN.CH.2015.07.en
- 837 Savini, A., Vertino, A., Marchese, F., Beuck, L., Freiwald, A., 2014. Mapping Cold-Water Coral
838 Habitats at Different Scales within the Northern Ionian Sea (Central Mediterranean): An
839 Assessment of Coral Coverage and Associated Vulnerability. *PLoS One* 9, e87108 EP –.
840 doi:10.1371/journal.pone.0087108
- 841 Sánchez, F., González-Pola, C., Druet, M., García-Alegre, A., Acosta, J., Cristobo, J., Parra, S., Ríos,
842 P., Altuna, Á., Gómez-Ballesteros, M., Muñoz-Recio, A., Rivera, J., del Río, G.D., 2014. Habitat
843 characterization of deep-water coral reefs in La Gaviara Canyon (Avilés Canyon System,
844 Cantabrian Sea). *Deep Sea Res. Part II Top. Stud. Oceanogr.* 106, 118–140.
845 doi:10.1016/j.dsr2.2013.12.014
- 846 Scales, K.L., Miller, P.I., Ingram, S.N., Hazen, E.L., Bograd, S.J., Phillips, R.A., Thuiller, W., 2016.
847 Identifying predictable foraging habitats for a wide-ranging marine predator using ensemble
848 ecological niche models. *Divers. Distrib.* 22, 212–224. doi:10.1111/ddi.12389

- 849 Schneider, A., Wallace, D.W.R., Körtzinger, A., 2007. Alkalinity of the Mediterranean Sea. *Geophys*
850 *Res Lett* 34, 285. doi:10.1029/2006GL028842
- 851 Seo, C., Thorne, J.H., Hannah, L., Thuiller, W., 2009. Scale effects in species distribution models:
852 implications for conservation planning under climate change 5, 39–43.
853 doi:10.1098/rsbl.2008.0476
- 854 Simoncelli, S., Fratianni, C., Pinaridi, N., Grandi, A., Drudi, M., 2019. Mediterranean Sea Physical
855 Reanalysis (CMEMS MED-Physics)[Data set]. Copernicus Monitoring Environment Marine
856 Service (CMEMS). doi:https://doi.org/10.25423/MEDSEA_REANALYSIS_PHYS_006_004
- 857 Soetaert, K., Mohn, C., Rengstorf, A.M., Grehan, A., van Oevelen, D., 2016. Ecosystem engineering
858 creates a direct nutritional link between 600-m deep cold-water coral mounds and surface
859 productivity. *Sci Rep* 6, 35057 EP –. doi:10.1038/srep35057
- 860 Taviani, M., Angeletti, L., Canese, S., Cannas, R., Cardone, F., Cau, A., Cau, A.B., Follesa, M.C.,
861 Marchese, F., Montagna, P., Tessarolo, C., 2017. The “Sardinian cold-water coral province” in
862 the context of the Mediterranean coral ecosystems. *Deep Sea Res. Part II Top. Stud. Oceanogr.*
863 145, 61–78. doi:10.1016/j.dsr2.2015.12.008
- 864 Taviani, M., Angeletti, L., Cardone, F., Montagna, P., Danovaro, R., 2019a. A unique and threatened
865 deep water coral-bivalve biotope new to the Mediterranean Sea offshore the Naples megalopolis.
866 *Sci Rep* 9, 3411. doi:10.1038/s41598-019-39655-8
- 867 Taviani, M., Angeletti, L., Fogliini, F., Corselli, C., Nasto, I., Pons-Branchu, E., Montagna, P., 2019b.
868 U/Th dating records of cold-water coral colonization in submarine canyons and adjacent sectors
869 of the southern Adriatic Sea since the Last Glacial Maximum. *Prog. Oceanogr.* 175, 300–308.
870 doi:10.1016/J.POCEAN.2019.04.011
- 871 Teruzzi, A., Bolzon, G., Cossarini, G., Lazzari, P., Salon, S., Crise, A., Solidoro, C., 2019.
872 Mediterranean Sea Biogeochemical Reanalysis (CMEMS MED-Biogeochemistry) [Data set].
873 Copernicus Monitoring Environment Marine Service (CMEMS).
874 doi:https://doi.org/10.25423/MEDSEA_REANALYSIS_BIO_006_008
- 875 Thuiller, W., Bruno, L., Robin, E., Araújo, M.B., 2009. BIOMOD – a platform for ensemble forecasting
876 of species distributions. *Ecography* 32, 369–373. doi:10.1111/j.1600-0587.2008.05742.x
- 877 Turner, M.G., Arthaud, G.J., Engstrom, R.T., Hejl, S.J., Liu, J., Loeb, S., McKelvey, K., 1995.
878 Usefulness of spatially explicit population models in land management. *Ecol. Appl.* 5, 12–16.
879 doi:10.2307/1942046
- 880 Turner, J.A., Babcock, R.C., Hovey, R., Kendrick, G.A., 2018. Can single classifiers be as useful as
881 model ensembles to produce benthic seabed substratum maps? *Estuar Coast Shelf Sci* 204,
882 149–163. https://doi.org/10.1016/j.ecss.2018.02.028
- 883 Tursi, A., Mastrototaro, F., Matarrese, A., Maiorano, P., D'Onghia, G., 2004. Biodiversity of the white
884 coral reefs in the Ionian Sea (Central Mediterranean) 20, 107–116.
885 doi:10.1080/02757540310001629170
- 886 Valverde, A.J., Lobo, J.M., Hortal, J., 2008. Not as good as they seem: the importance of concepts in
887 species distribution modelling. *Divers. Distrib.* 14, 885–890. doi:10.1111/j.1472-
888 4642.2008.00496.x
- 889 Van den Beld, I.M.J., Bourillet, J.-F., Arnaud-Haond, S., de Chambure, L., Davies, J.S., Guillaumont,
890 B., Olu, K., Menot, L., 2017. Cold-water coral habitats in submarine canyons of the Bay of Biscay.
891 *Front. Mar. Sci.* 4, 279. doi:10.3389/fmars.2017.00118
- 892 Vierod, A.D.T., Guinotte, J.M., Davies, A.J., 2014. Predicting the distribution of vulnerable marine
893 ecosystems in the deep sea using presence-background models. *Deep Sea Res. Part II Top.*
894 *Stud. Oceanogr.* 99, 6–18. doi:10.1016/j.dsr2.2013.06.010
- 895 Wisz, M.S., Hijmans, R.J., Li, J., Peterson, A.T., Graham, C.H., Guisan, A., Group, N.P.S.D.W., 2008.
896 Effects of sample size on the performance of species distribution models. *Divers. Distrib.* 14,
897 763–773. doi:10.1111/j.1472-4642.2008.00482.x
- 898 Zhang, L., Liu, S., Sun, P., Wang, T., Wang, G., Zhang, X., Wang, L., 2015. Consensus Forecasting
899 of Species Distributions: The Effects of Niche Model Performance and Niche Properties. *PLoS*
900 *One* 10, e0120056 EP –. doi:10.1371/journal.pone.0120056
- 901 Zibrowius, H., 2003. The “White Coral Community,” canyon and seamount faunas of the deep
902 Mediterranean Sea. RAC/SPA - Regional Activity Centre for Specially Protected Areas.
- 903 Zweng, M.M., Reagan, J.R., Antonov, J.I., Locarnini, R.A., Mishonov, A.V., Boyer, T.P., Garcia, H.E.,
904 Baranova, O.K., Johnson, D.R., Seidov, D., Biddle, M.M., 2013. World ocean atlas 2013. volume
905 2, salinity. NOAA Atlas NESDIS 74.
- 906

Highlights

- We mapped the potential distribution of *Lophelia pertusa* in the Mediterranean Sea
- We provide uncertainty estimates for the model predictions
- Mediterranean colonies are subjected to challenging environmental conditions
- The most suitable areas occur in the continental slope of the west and central basins
- The overlap of the Mediterranean MPAs with the most suitable areas is limited

Journal Pre-proof

Declaration of interests

The authors declare that they have no known competing financial interests or personal relationships that could have appeared to influence the work reported in this paper.

The authors declare the following financial interests/personal relationships which may be considered as potential competing interests:

Journal Pre-proof